Impact of DNA Damage on the Contractile Function of Cardiomyocytes

Submitted by

Ingrid Petersen

Bioengineering

To

The Honors College

Oakland University

In partial fulfillment of the

requirement to graduate from

The Honors College

Mentor: Colin Wu, PhD, Professor of Biochemistry

Department of Chemistry

Oakland University

December 3rd, 2021

Table of Contents

Abstract

The accumulation of reactive oxygen species (ROS) has detrimental effects on heart muscle cells, including cellular apoptosis and dysfunction that contribute to the progression of cardiovascular diseases. Additionally, ROS can modify bases to form DNA lesions, leading to genetic instability and mutations. Other types of DNA damage occur when cells are exposed to mutagenic agents leading to single-stranded (SSB) and double-stranded (DSB) breaks. Although oxidative stress and ROS can negatively affect heart muscle function and cause DNA damage, the impact of oxidative DNA damage on contractile function remains poorly understood. The purpose of this project is to determine the sensitivity of cardiomyocyte contractile mechanics in response to SSBs, DSBs, and ROS. The relationship between DNA damage and cardiomyocyte activity is examined by measuring the relative abundance of SSBs and DSBs through a Comet assay in coordination with video-based analysis to evaluate contractile function of mouse HL-1 cells. In the presence of hydrogen peroxide, contraction rate increased in response to a mild amount of damage but decreased under high levels. This suggests that cardiomyocyte function is stimulated by oxidative stress until severe damage debilitates cellular processes. Subsequent conditions of camptothecin (SSB) and bleomycin (DSB) were employed to illuminate the role of specific types of DNA damage. These results indicate that DSBs contribute toward contractile function more significantly than do SSBs. Future directions include expanding these results to a human cardiac model system, such as human induced pluripotent stem cell-derived cardiomyocytes (hiPS-CM) and the application of an enzyme-modified alkaline comet assay to further investigate the contribution of oxidative DNA damage on heart cell activity.

Introduction

It is essential that genome integrity is preserved to maintain cell function. Endogenous and exogenous reactive oxygen species carry the potential to cause DNA damage. DNA damage is considered a change in the structure of DNA that modifies its expected function or coding abilities in transcription or replication [1]. This commonly takes the form of a DNA lesion, which could be a base alteration or deletion, sugar alteration or breaks to the DNA strand [2]. DNA lesions can block genome transcription and may become a permanent alteration to the strand if not repaired prior to replication. DNA lesions can occur through necessary physiological processes. For example, DNA base substitutions may originate from mismatches occurring during replication. Similarly, DNA strand breaks may take place as a result of the mechanisms involved in removing DNA supercoils. Lastly, oxidative DNA damage may arise from exposure to reactive oxygen species that are present as a result of oxidative respiration [3]. This paper will focus on single-strand and double-strand DNA breaks as well as oxidative DNA damage.

The type of DNA damage that occurs most frequently are single-strand DNA breaks (SSBs). These breaks consist of a nick to a single strand of the phosphate backbone of DNA. SSBs can originate as an intermediate during base-excision repair of damaged bases or abasic sites as well as through the disintegration of oxidized ribose. Lastly, inappropriate or clustered cleavage from DNA topoisomerase 1 during DNA transcription and replication can lead to SSBs. The outcome of chromosomal SSBs can block or cause replication forks to collapse, which could further produce DSBs [4]. Additionally, high levels of SSBs can lead to genetic instability and

cell death. Greater evidence suggests the role of SSBs in cancer, neurodegenerative diseases and heart failure [5].

Double-strand DNA breaks (DSBs) occur less frequently but have more severe consequences, leading to cell death if left unrepaired. Double-strand breaks are defined as the separation of the phosphate backbone on both sides of the double helix in close proximity to each other. When this occurs, base pairing is interrupted and the free ends of the double helix are allowed to physically separate from each other, creating difficulties in repair [6]. Ionizing radiation (IR) and ultraviolet light (UV) are prevalent DNA-damaging agents that can initiate DSBs. DSBs can originate inadvertently from base excision repair mechanisms when DNA damage occurs simultaneously on both strands. Additionally, DSBs can be produced in DNA replication when a polymerase encounters a SSB and stalls, causing the replication fork to collapse which creates DSBs in the process. The consequences of DSBs include mutations and chromosomal rearrangements that can lead to cell death and cancer [7].

DNA damage may also arise from interactions with reactive oxygen species (ROS) that are generated as a byproduct of oxidative phosphorylation. Oxidative phosphorylation utilizes the electron transport system to extract energy from the movement of electrons with oxygen acting as the final electron acceptor. Intracellular oxygen is broken down into superoxide radicals (•O2–) by NADH hydrogenase 2. The superoxide ions are then able to degrade to hydrogen peroxide (H_2O_2) which can catalyze an additional reaction with iron to generate a hydroxyl radical (•OH). When there is an excess of reactive oxygen species in the cell, oxidative DNA damage will occur as a result of their ability to strip DNA, RNA, proteins and lipids of their electrons [8]. The nucleotide base guanine is particularly susceptible to oxidative DNA damage

due to its low oxidation potential. The reactive oxygen species are able to modify the nucleotide residues of guanine to produce 8-oxo-7,8-dihydroguanine (8-oxoG) [9]. In addition to cytosine, 8-oxoG is able to base pair with adenine which introduces a transversion mutation. This relationship is shown in figures 1 and 2 below. In addition to causing DNA base lesions, ROS are able to target the phosphate backbone of DNA and induce both single-strand and double-strand breaks [10]. Overall, the detrimental effects of oxidative DNA damage is reflected by the introduction of SSBs and DSBs as well as the modification and mispairing of DNA bases, leading to genome instability and mutation.

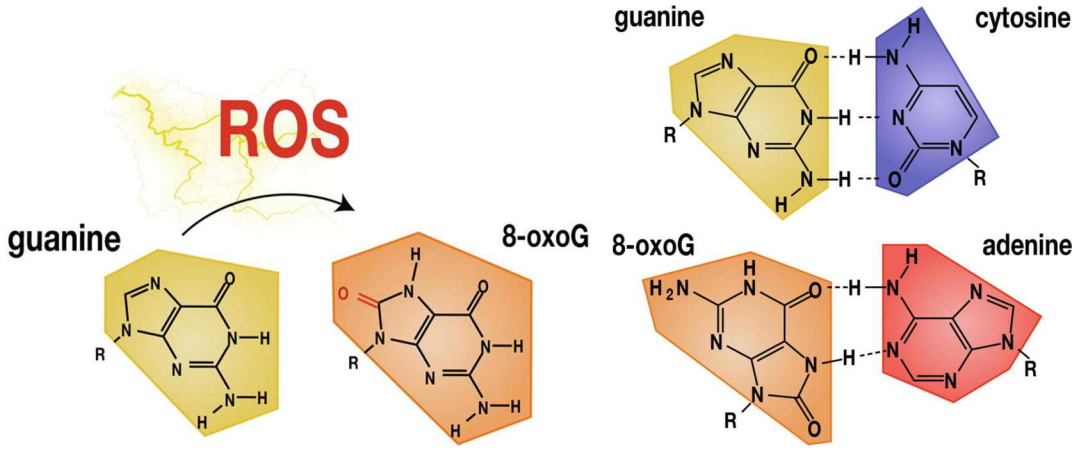

Figures 1 & 2: *Figure 1 (left) shows guanine in the presence of reactive oxygen species (ROS) to produce 8-oxoG. Figure 2 (right) depicts the altered base pairing associated with the introduction of 8-oxoGs. Images provided by Poetsch (2020).*

Current Research

Oxidative stress is characterized by the excess of reactive oxygen species compared to antioxidant production within a cell. The effect of oxidative stress on heart health and function has been extensively studied [11-14]. Elevated ROS causes cellular apoptosis and dysfunction as well as affecting cell migration, and proliferation. The previously mentioned factors combined with the stimulatory effect of ROS on inflammatory mediators and signaling molecules, results in an active role of ROS in tissue remodeling. Cardiac remodeling involves changes in the structure and function of cardiomyocytes as well as alterations in the extracellular matrix driven by the proliferation of cardiac fibroblasts. This results in modifications to the shape and volume of the heart, commonly occurring following myocardial infarction. Specifically, oxidative stress has been implicated in myocardial remodeling and heart failure. In a failing heart, high levels of ROS prompt greater ROS generation that further contribute to the disease progression. Likewise, lipid peroxidation and mitochondrial damage and dysfunction provoke greater ROS generation [15]. Similarly, the role of oxidative stress and inflammation in the progression of heart failure was explored through the article by Aimo et al [16]. Impacts of oxidative stress resulted in altered Ca^{2+} regulation, cardiac hypertrophy, initiation of apoptosis and the inflammatory response, all of which are associated with aspects of the progression of heart failure. Another indicator of heart function is through contractile mechanics. The study by Zima & Blatter found that ROS affected contractile ability through the redox-modulation of proteins involved in cardiac excitation and contraction [17]. Proteins of cointerest included Ca^{2+} channels and transporters, such as Ca^{2+} ATPase that when oxidized inhibited uptake of Ca^{2+} into the sarcoplasmic reticulum, affecting contractile function. The contribution of DNA damage in a failing heart is examined by Higo et al. [18]. The accumulation of single strand DNA breaks are

suggested to play a role in the mechanism of heart failure by inducing the DNA damage response. This response leads to inflammation which can, if persistent, cause cardiac remodeling, a key characteristic in the development in heart failure. The article proposed by Zhang et al. introduces cardiomyocyte dysfunction resulting from oxidative DNA damage [19]. This study found that oxidative DNA damage stimulated excessive poly(ADP)-ribose polymerase 1 (PARP1) activity. This led to tachypacing dysfunction of the atria as well as further inducing DNA damage and contractile dysfunction due to the depletion of NAD+ by PARP1 activity. They found that the cardiomyocytes of patients with persistent atrial fibrillation represented high levels of DNA damage and correlating PARP1 activity, suggesting that PARP1 inhibition would serve as a potential therapeutic target to maintain heart function. A related direction will be elaborated upon within this paper to expand the intersection of oxidative stress and DNA damage within cardiac contractile function.

Aims and Objectives

Introduction

The examination of how DNA damage affects heart cell contractile function is relevant in the consideration of the progression of heart diseases. Uncovering the impact of DNA damage on the heart would contribute to a greater understanding of the mechanisms and treatment for heart failure. This can be achieved by applying the quantification of specific types of DNA damage to the evaluation of oxidative stress on contractile function, highlighting the association between DNA damage and cell function.

Aims

1. To categorize the profile of DNA damage induced by oxidative stress.

2. To determine the impact of oxidative stress on the contractile function of cardiomyocytes.

3. To correlate the relationship between specific types of DNA damage and contractile function.

4. To compare the profile and contractile function of DNA damage for single-strand and double-strand breaks to oxidative stress.

Objectives

1. Oxidative stress has been shown to generate DNA damage within cells. By quantifying the degree of resulting DNA damage, it can then be concluded that specific conditions of oxidative stress will correlate to a known amount of DNA damage. These controls can be utilized as a method to study the effect of DNA damage in cells.

2. The contractile function of cardiomyocytes can be characterized as a consequence of varying levels of oxidative stress, allowing the impact oxidative stress on the functionality of the cell to be isolated. This provides insight into the limits of oxidative stress that cardiomyocytes are be able to sustain before function is lost

3. The DNA damage profile can be applied to the conditions of oxidative stress used to measure contractile function. Consequently, the influence of DNA damage on cardiomyocyte contractile function can be explored. This synthesis allows the susceptibility of cardiomyocytes to DNA damage to be determined, enabling greater analysis of the effects of DNA damage on the heart.

4. Camptothecin and bleomycin can be used as chemical agents to induce single-strand and double-strand DNA breaks respectively. The resulting DNA damage profile for SSBs and DSBs can be characterized alongside their affected contractile function. This provides insight that can be contrasted with the evaluation of oxidative stress to establish the specific types of DNA damage affecting contractile function.

Materials and Methods

Cell Culture and Passaging:

The *in vitro* model for heart cell contractile function that was selected for this experiment were HL-1 cells, a cardiac muscle cell line that is derived from AT-1 mouse atrial cardiomyocyte tumor lineage [20]. These cells were chosen for their unique characteristics, most notable is their ability to spontaneously contract and be repeatedly passaged [21]. It is important that the differentiated phenotype is still observed following serial propagation, and HL-1 cells have been shown to "maintain cardiac morphological, biochemical, and electrophysiological properties" [22].

In order to ensure the greatest degree of reliability in this experiment, trials were conducted with 6 replicate wells for each condition for measures of contractility and 500-1000 cells for measures of DNA damage. Additionally, all experiments were performed on cells at the same passage number, passage 6, to minimize the effect of surplus DNA damage accumulated through culturing conditions. This was determined to be a necessary requirement due to the high sensitivity and susceptibility of cardiomyocytes to DNA damage as the passage number increased. Furthermore, all trials of the same treatment were completed simultaneously to minimize uncontrollable variables between conditions.

Protocols:

Plate/Flask Preparation

1. Add 1 mL of Fibronectin/Gelatin to each well of a 6-well plate. (3 mL for a T-25, 4 mL for a T-75)

a. Fibronectin/Gelatin (200 mL)

i. .02% Gelatin Solution- 50 mg Gelatin in 250 mL Type 1 water.

ii. Autoclave .02% Gelatin Solution and let cool.

iii. Add 500 µL of 2 mg/mL Fibronectin to 200 mL of Gelatin Solution.

iv. Sterile filter with 0.22 µm filter.

v. Aliquot as necessary and store in -20°C freezer.

2. Let flasks sit in Fibronectin/Gelatin overnight at 4°C or for 1 hour at 37°C.

Passaging

1. Change HL-1 Expansion Media daily until cells have reached confluency.

a. HL-1 Expansion Media (500 mL)

i. 435 mL Claycomb Basal Medium

ii. 50 mL HL-1 Qualified FBS

iii. 5 mL 10 mM Norepinephrine

iv. 5 mL 200 mM L-Glutamine

v. 5 mL 100x Penicillin/Streptomycin

2. When confluent, cells must be split. Start by placing HL-1 Media and 0.25% trypsin in a water bath for 30 minutes at 37°C.
3. Aspirate Media from T-25 containing cells.
4. Rinse with 5 mL of PBS then aspirate.
5. Add 1 mL of Trypsin, let sit for 2 minutes in 37°C incubator.

a. After 2 minutes, check for cell detachment under microscope.

6. Add 1 mL of Trypsin inhibitor to flask.

a. Trypsin Inhibitor (50 mL)
    i. 12.5 mg Trypsin inhibitor
    ii. 50 mL PBS
    iii. Sterile filter with 0.22 μm filter.

7. Add 2 mL of cell, Trypsin/Trypsin Inhibitor solution into a 15 mL conical tube.
8. Rinse T-25 flask with 3 mL of HL-1 Media and add to previous 15 mL tube.
9. Centrifuge cells at 500 rpm for 5 minutes.
    a. During the 5 minutes: Aspirate off the Fibronectin/Gelatin mixture from the fresh flask or plate.
    b. Add HL-1 media to plate or flask. (2 mL for each well of a 6-well plate and 4 mL for a T-25)
10. Gently aspirate the media from the 15 mL tube without disturbing the cell pellet.
11. Resuspend in 3 mL of HL-1 Media, add cells to flasks/plate in a 1:3 split ratio.

Experimental Reagents:

Hydrogen peroxide, camptothecin and bleomycin will be used as reagents to induce DNA damage through measurable, exogenous methods. The treatment of cardiomyocyte cells in varying concentrations of hydrogen peroxide provides a method to induce oxidative stress. Hydrogen peroxide is selected out of many reactive oxygen species (ROS) that inflict DNA damage due to its convenience and ability to generate both double and single stranded DNA breaks. This allows the role of the specific types of DNA damage in contractile function to be explored.

Similarly, camptothecin and bleomycin are known mutagenic agents in producing single-strand DNA breaks and double-strand DNA breaks, respectively. Camptothecin is a quinolone

alkaloid that has been used as a chemotherapeutic agent due to its ability to inhibit DNA topoisomerase 1. Specifically, the cleavage complex of the topoisomerase is stabilized while the re-ligation breaks are hindered. This results in the generation of DNA single-strand breaks in the genome that are left un-ligated [23]. This makes camptothecin an ideal candidate to induce SSBs in cells. Bleomycin similarly has applications as a chemotherapeutic agent, acting as a radiomimetic compound by generating double-strand breaks directly [7]. This occurs since activated bleomycin contains a reduced transition metal and oxygen, which in the presence of an electron reductant initiates a C-H bond cleavage [24]. The use of bleomycin allows the induction and investigation of DSBs in DNA.

Hydrogen Peroxide Treatment

Cells were exposed to different concentrations of hydrogen peroxide (control, 100 uM, 300 uM) for 24 hours.

Bleomycin Treatment

Cells were exposed to different concentrations of bleomycin (control, 1 ug/mL, 10 ug/mL, 50 ug/mL, 75 ug/mL, 100 ug/mL) for 15 minutes.

Camptothecin Treatment

Cells were exposed to different concentrations of camptothecin (control, DMSO control, 1 ug/mL, 10 ug/mL, 50 ug/mL, 100 ug/mL, 200 ug/mL) for 15 minutes.

Comet Assay:

Once DNA damage is induced within cells, the relative abundance of single-strand and double-strand DNA breaks can be measured through a comet assay. While PCR is another common method used to measure DNA damage, it is typically used for gene-specific DNA damage and cannot quantify or determine the type of damage present. Alternatively, the comet assay is well suited for analysis within individual cells and depending on the conditions, neutral or alkaline, double stranded and single stranded breaks can be detected [25]. Another method that is employed to measure the presence of DNA damage is γ-H2AX. Following the induction of double-strand breaks, the nucleosome packaging protein histone H2A variant, H2AX, becomes phosphorylated. The presence of the phosphorylated form, γ-H2AX, is identified through the use of fluorescent antibodies [26]. However, this approach was not selected due to its indirect method of evaluating DNA damage. While γ-H2AX measurements rely on the detection of proteins involved in DNA damage repair, the comet assay assesses DNA damage directly.

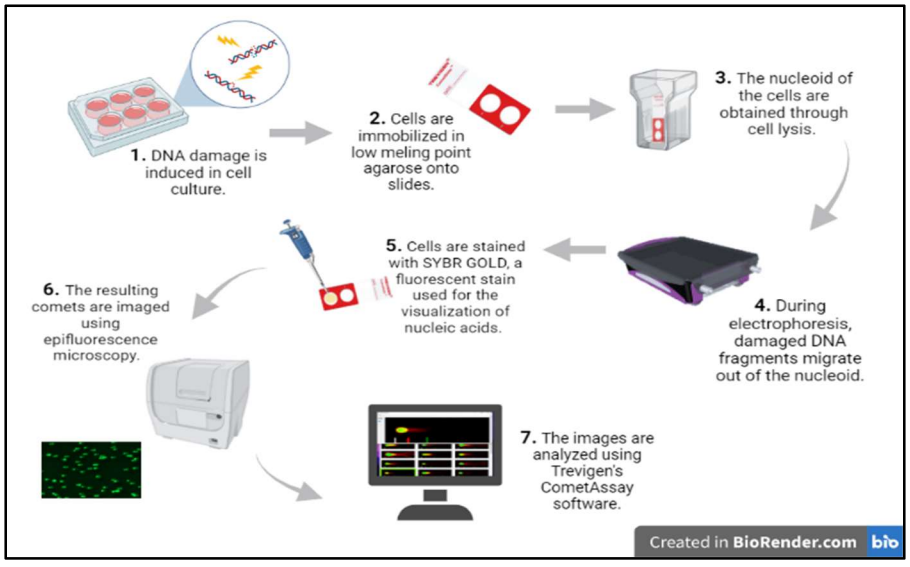

Figure 3: *A step by step overview of the comet assay procedure.*

A comet assay is a single cell gel electrophoresis assay that is intended to show the presence of DNA strand breaks based on differences of migration when current is applied. As shown in the overview above, the cells are immobilized in low melting agarose onto slides following the induction of DNA damage. Next, the cells are lysed so that the nucleus of the cell can be exposed to electrophoresis. In the alkaline assay, cells are additionally treated to unwind and denature the DNA. This enables a more sensitive test and allows the Alkaline assay to detect both SSBs and DSBs. The Neutral assay is used solely for the detection of DSBs.

The comet assay operates on the principle that undamaged DNA tends to move slower and remain within the nucleus while damaged DNA will move more rapidly and form a tail trailing from the nucleus. Analysis of the intensity of the tail determines the amount of DNA damage present. The two most reliable indicators of DNA damage are the DNA percentage located in the tail and the tail moment. The DNA percentage in the tail corresponds to the amount of DNA content in the tail as a percentage of total comet DNA content. The tail moment incorporates the length of DNA migration and is calculated as the tail length multiplied by the tail DNA percentage. The tail moment is particularly relevant to the Neutral assay since the migration distance is proportional to increasing levels of DNA damage.

Cell and Slide Preparation

1. Aspirate HL-1 media from the pre-treated wells and rinse with PBS.
2. Collect cells with the use of Accutase to detach cells from plate.
3. Centrifuge cells and re-suspend in PBS to rinse cells of treatment containing media.
4. Centrifuge again and remove excess PBS.

5. Use a cell count to determine the dilution volume of PBS to add to the cell solution. The desired concentration is 1 x 10^5 cells/mL.
6. Combine 50 µL of PBS cell solution to 500 µL of Low-Melt Agarose. Cover the sample area of Trevigen Comet Assay slides with cell-agarose mixture.
7. Allow agarose to gel for 10 minutes at 4°C in the dark.
8. Proceed with either the Alkaline or Neutral comet assay protocol.

Alkaline Assay

The Trevigen Alkaline Comet Assay protocol was followed for this experiment.

1. Cool lysis solution at 4°C for at least 20 minutes beforehand. After the last step of the cell preparation section, place the slides into Lysis Solution for 30-60 minutes at 4°C.
2. Place slides in Alkaline Unwinding Solution in the dark for 20 minutes at room temperature or for 1 hour at 4°C.
    a. Alkaline Unwinding Solution (100 mL)
        i. 0.8 g NaOH Pellets
        ii. 500 µL 200 mM EDTA
        iii. 99.5 mL Type 1 water
3. Run electrophoresis in Alkaline Electrophoresis Solution at 4°C set to 21 volts, 500 mA for 40 minutes.
    a. Alkaline Electrophoresis Solution (1 L)
        i. 8 g NaOH Pellets
        ii. 2 mL 500 mM EDTA, pH 8
        iii. 1 L Type 1 water (add up to 1 L after NaOH has dissolved)

4. Rinse slide by immersion in Type 1 water for 5 minutes at room temperature. Repeat again.
5. Place slide in 70% Ethanol for 5 minutes at room temperature.
6. Dry samples at 37°C for 10-15 minutes. Slides may also be dried in a desiccant overnight.

Neutral Assay

The Trevigen Neutral Comet Assay protocol was followed for this experiment.

1. Cool lysis solution at 4°C for at least 20 minutes beforehand. After the last step of the cell preparation section, place the slides into Lysis Solution for 1 hour at 4°C.
2. Place slides in 1x Neutral Electrophoresis Buffer for 30 minutes at 4°C.
    a. 1x Neutral Electrophoresis Buffer (1 L)
        i. Dilute 100 mL of 10x Neutral Electrophoresis Buffer in 900 mL of Type 1 water.
    b. 10x Neutral Electrophoresis Buffer (500 mL)
        i. 60.57 g Tris Base (mol. wt. = 121.14)
        ii. 204.12 g Sodium Acetate (mol. wt. = 136.08)
        iii. Adjust to pH=9 with glacial acetic acid
3. Run electrophoresis in Neutral Electrophoresis Buffer at 4°C set to 21 volts, 500 mA for 40 minutes.
4. Immerse slides in DNA Precipitation Solution for 30 minutes at room temperature.
    a. DNA Precipitation Solution (100 mL)
        i. 13.4 mL 7.5 M Ammonium Acetate (NH_4Ac - mol. wt=77.08)

ii. 95% EtOH

b. 7.5 M Ammonium Acetate (15 mL)

i. 8.67 g NH_4Ac (mol. wt=77.08)

ii. 15 mL Type 1 water (add up to 15 mL after NH_4Ac has dissolved)

5. Place slide in 70% Ethanol for 30 minutes at room temperature.
6. Dry samples at 37°C for 10-15 minutes. Slides may also be dried in a desiccant overnight.

Staining and Imaging

After the comet assay is completed, DNA visualization is conducted with the use of a fluorescent stain, SYBR Gold, viewed and imaged by epifluorescence microscopy using a Cytation Cell Imaging Multi-Mode Reader.

1. SYBR Gold solution is applied to cover the sample area of the slides. Let sit for 30 minutes in the dark.

a. SYBR Gold (30 mL)

i. 1 µL SYBR Gold Nucleic Acid Gel Stain (10,000X Concentrate in DMSO)

ii. 30 mL TE buffer

iii. Sterile filter with 0.22 µm filter

b. TE buffer (30 mL)

i. 300 µL 10 mM Tris-HCl pH 7.5

ii. 60 µL 1 mM EDTA

iii. 29.64 mL Type 1 water

2. Gently rinse excess stain off of slides with water.
3. Dry samples at 37°C for 10-15 minutes.
4. Image immediately after samples are completely dry.

Analysis

The comet images were analyzed using the Trevigen Comet Analysis Software. The image processing software automatically locates and scores the comets. The accuracy of the data is further refined by manually adjusting the nucleus and comet tail parameters individually by comet. Example images of adjusting nucleus and tail parameters are provided in the appendix. The percentage of DNA in the tail and the tail moment are evaluated to assess the amount of DNA damage for each condition.

Contractile Function:

Contractile function is dependent upon calcium ions to couple the electrical excitation of the cell to a physical muscle contraction. The action potentials of cardiac contraction are propagated to neighboring cells through the depolarization of membrane potential resulting from the movement of ions, including Ca^{2+}, in or out of the cell. When the threshold of around -40 mV is reached, calcium channels open allowing Ca^{2+} to flow into the cell [27]. These calcium ions are necessary for muscle contraction by the sliding filament mechanism. This occurs as Ca^{2+} binds to troponin, which shifts tropomyosin to expose myosin binding sites, enabling muscle contraction to proceed through cross-bridge cycling [28].

As a result of this mechanism, contractile function can be assessed by measuring the influx of Ca^{2+}. Fluo-8 am was selected as a calcium binding dye to measure the amount of

intracellular calcium in the cell. The fluorescence of the dye is amplified when binding to calcium occurs. Therefore, the intensity of measured fluorescence increases as intracellular calcium levels increase, which corresponds to cell contraction.

The intensity of fluorescence is recorded over time using a Cytation Cell Imaging Multi-Mode Reader fluorescence microscope. The intensity peak profile is analyzed using Matlab to identify the time between peaks so that the average beats per minute for each sample can be calculated. The calculation of beats per minute is used to compare the effects of the selected chemical reagents on the contractile function of HL-1 cells. The Matlab script and sample equations used to obtain the beats per minute data are provided in the appendix.

Staining and Imaging

The protocol for detection of spontaneous calcium fluctuations in confluent HL-1 cells provided by MilliporeSigma was followed.

1. HL-1 cells are grown to 100% confluency and are exposed to DNA-damage inducing treatments.
2. Prepare a 100x Fluo-8 AM stock solution.
    a. <u>100x Fluo-8 AM</u>
        i. 50 µg Fluo-8 AM (AAT Bioquest Cat. No. 21081)
        ii. 100 µL DMSO
3. Aspirate treatment-containing media and rinse with Hepes Buffered Tyrode's Solution.
    a. <u>Hepes Buffered Tyrode's Solution (500 mL)</u>
        i. 11.9 mL 5 M NaCl
        ii. 833.33 µL 3 M KCl

iii. 1 mL 1 M $CaCl_2$

iv. 1 mL 1 M $MgCl_2$

v. 12.5 mL 1 M Hepes

vi. 3 g glucose

vii. Add up to 500 mL of Type 1 water

4. Aspirate Tyrode's solution and replace with 5 µM Fluo-8 AM Solution.
    a. 5 µM Fluo-8 AM Solution (6 mL) - dilute 100x Fluo-8 AM solution in a ratio of 1:10 in Tyrode's solution.
        i. 60 µL 100x Fluo-8 AM
        ii. 6 mL Tyrode's Solution
5. Incubate for 1 hour at 37°C.
6. Aspirate staining solution. Rinse with Tyrode's Solution.
7. Aspirate and replace with fresh Tyrode's Solution.
8. Immediately view and image the cells with the use of a fluorescence microscope.

Results

Comet Assay:

Hydrogen Peroxide-

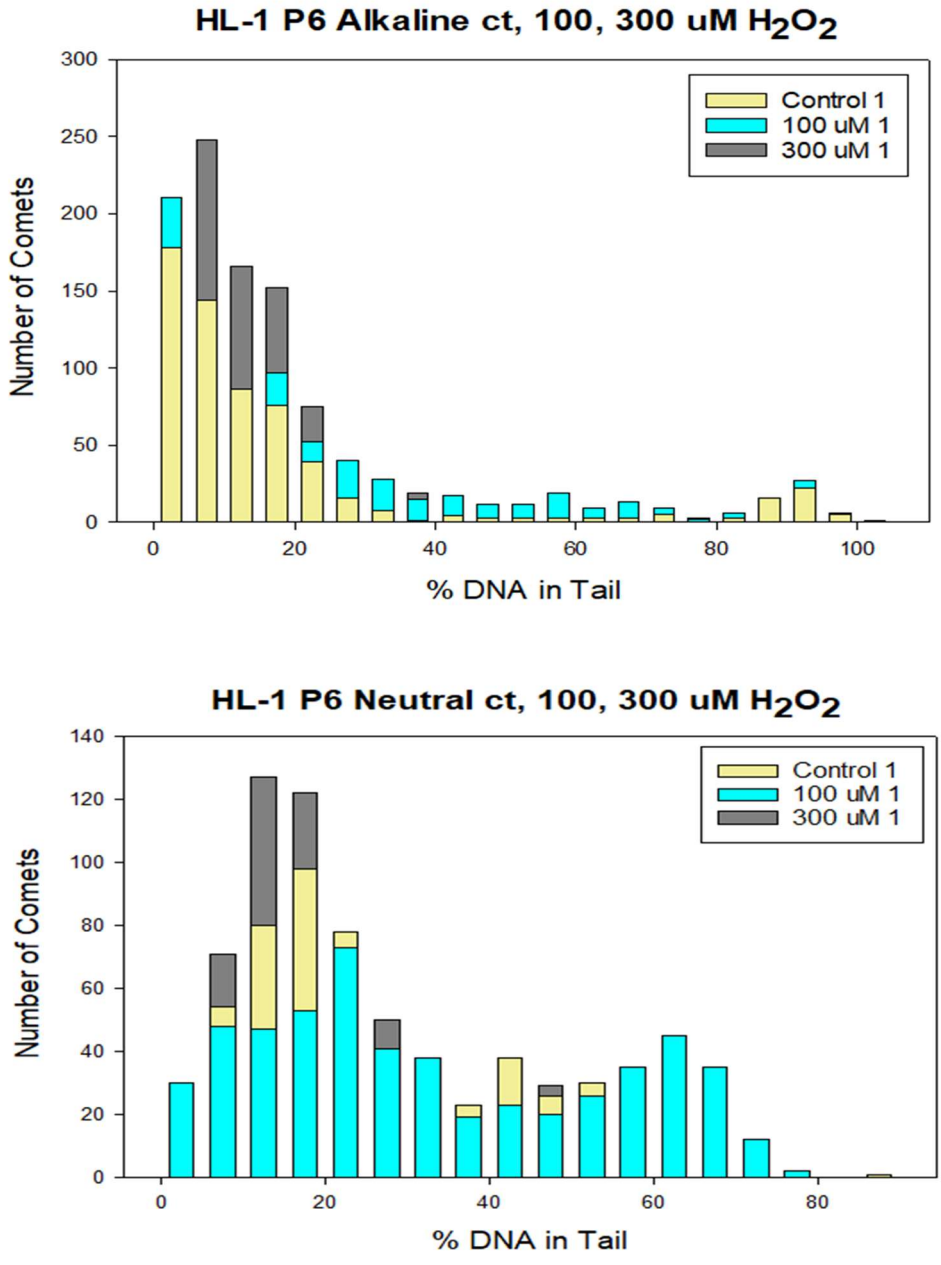

Figures 4 & 5: *The distribution of alkaline comets (top, figure 4) and neutral comets (bottom, figure 5) based on the percent DNA in the tail following the treatment with hydrogen peroxide.*

Hydrogen Peroxide Treatments	Alkaline % DNA in Tail	Neutral % DNA in Tail
Control	19.57 ± 16.55	31.07 ± 15.80
100 uM	19.09 ± 19.30	31.69 ± 18.02
300 uM	19.10 ± 12.79	29.41 ± 14.55

Table 1: *Results of the percent DNA in tail for alkaline and neutral comet assays following treatments with hydrogen peroxide.*

As is shown in Table 1, the percentage of DNA in the tail remains unchanged over varying concentrations of hydrogen peroxide. The baseline of DNA damage, as indicated by the control condition, is at a higher level for the Neutral comet assay rather than the Alkaline assay. Figures 4 & 5 show the distribution of the percentage of DNA in the tail for the comets in the Alkaline and Neutral comet assays with Hydrogen Peroxide treatment. The Alkaline comet shows the majority of the population of comets fall in the region of a low percentage of damage in the tail. The Neutral comet assay depicts a bimodal distribution where a sizable population of comet cells fall in the low damage region but a significant number of comets also lie in a higher damaged region. This distribution is important to note since the average alone would not provide an adequate representation of the data.

Bleomycin-

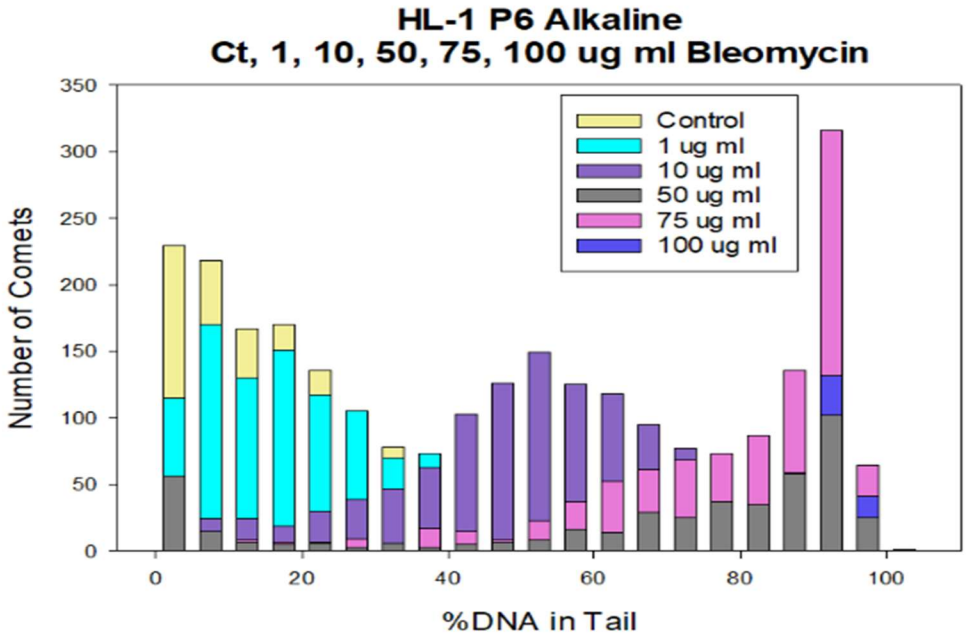

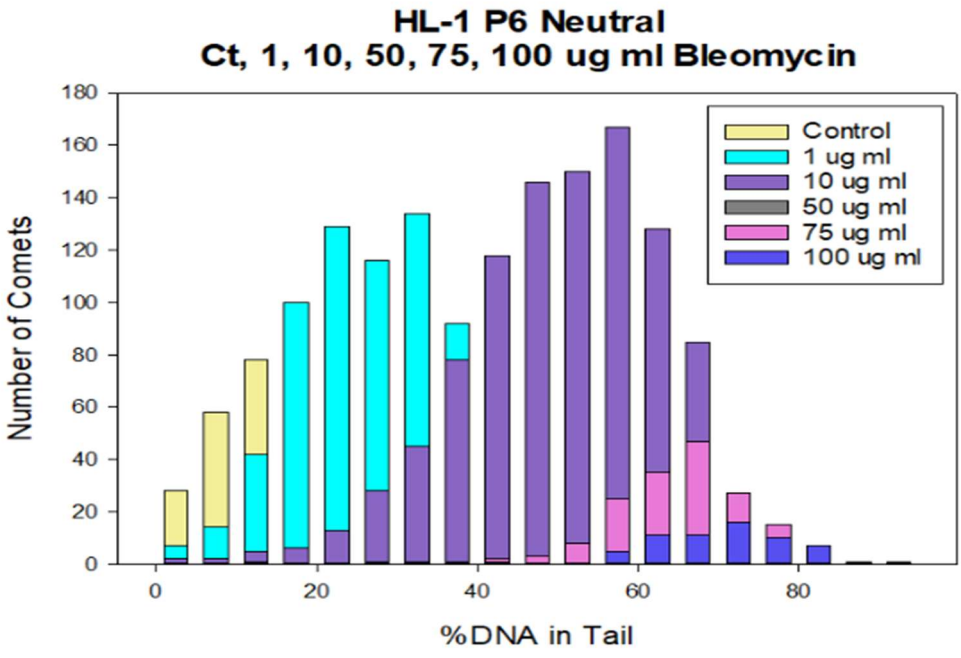

Figures 6 & 7: *The distribution of alkaline comets (top, figure 6) and neutral comets (bottom, figure 7) based on the percent DNA in the tail following the treatment with bleomycin.*

Bleomycin Treatments	Alkaline % DNA in Tail	Neutral % DNA in Tail
Control	24.39 ± 20.60	34.09 ± 19.12
1 ug/ml	27.72 ± 20.61	38.42 ± 16.55
10 ug/ml	53.03 ± 19.66	51.07 ± 12.48
50 ug/ml	65.35 ± 32.16	69.81 ± 6.27
75 ug/ml	76.82 ± 21.76	64.82 ± 9.26
100 ug/ml	79.77 ± 22.79	69.22 ± 8.64

Table 2: *Results of the percent DNA in tail for alkaline and neutral comet assays following treatments with bleomycin.*

Table 2 indicates the average percentage of DNA in the tail across the increase in concentration of bleomycin treatments. For the Alkaline assay, the data shows a steady increase in percentage of DNA in the tail as the concentration of bleomycin is increased. This indicates an increase in SSBs present in the HL-1 cells. In the Neutral assay, an increase in percentage of DNA in the tail, representative of DSBs, is shown as the treatment conditions are increased from 1 ug/ml and 10 ug/ml. At treatment levels greater than 50 ug/ml it appears that the percentage of DNA damage has reached a maximum amount and will plateau at that value regardless of further increases in bleomycin concentration. Figures 6 & 7 show the median of the distribution for each condition shifting to regions of higher DNA damage as bleomycin concentration is increased. It is important to eliminate the presence of an outlier group of a small number of highly damaged comets since they would have the potential to skew the average. The distribution shown in the histograms supports the concentration-dependent increase in DNA damage as indicated by the calculation of averages in the table.

Camptothecin-

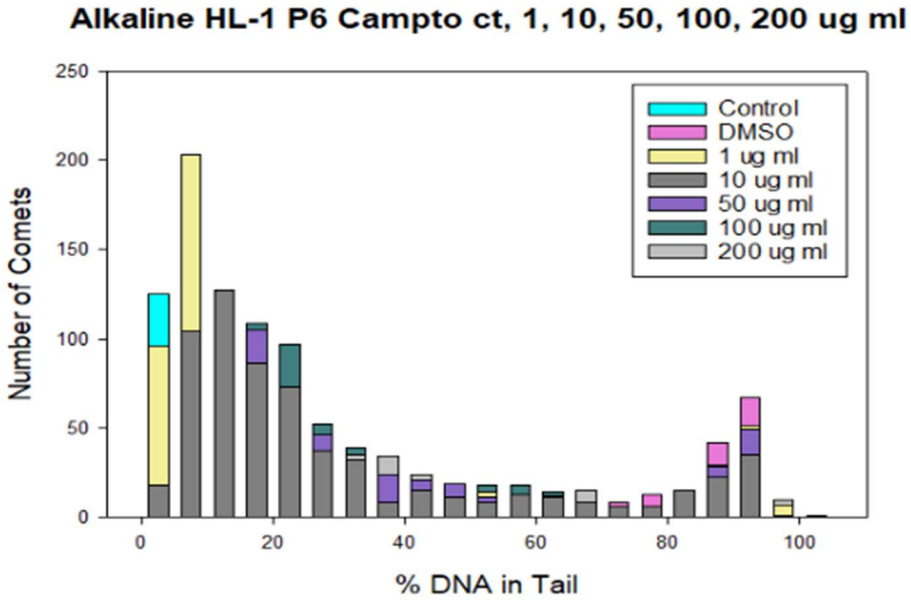

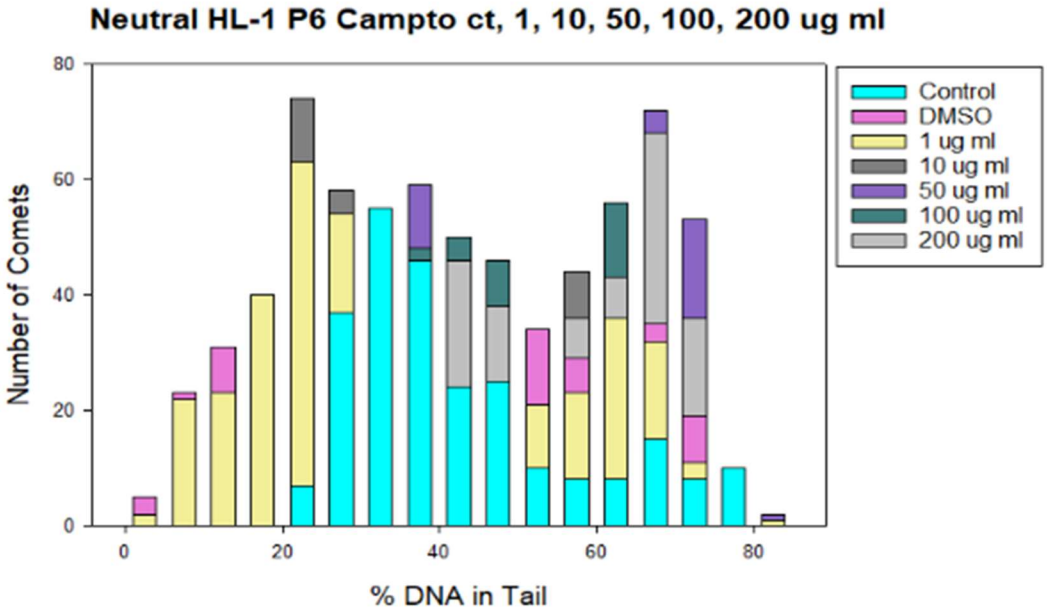

Figures 8 & 9: *The distribution of alkaline comets (top, figure 8) and neutral comets (bottom, figure 9) based on the percent DNA in the tail following the treatment with camptothecin.*

Camptothecin Treatments	Alkaline % DNA in Tail	Neutral % DNA in Tail
Control	20.31 ± 25.59	28.13 ± 20.11
DMSO	33.78 ± 32.92	40.18 ± 21.44
1 ug ml	25.88 ± 27.59	36.32 ± 19.22
10 ug ml	29.67 ± 26.47	38.31 ± 16.48
50 ug ml	36.20 ± 27.54	50.35 ± 16.02
100 ug ml	38.23 ± 27.28	49.71 ± 15.28
200 ug ml	45.13 ± 29.42	51.52 ± 14.41

Table 3: *Results of the percent DNA in tail for alkaline and neutral comet assays following treatments with camptothecin.*

Since the camptothecin treatments are provided in a solution of DMSO, an additional control condition of DMSO was included. This was incorporated to isolate the effects of camptothecin alone and to eliminate the contribution of DMSO. Table 3 shows the change in the percentage of DNA in the tail as the concentration of camptothecin is increased. Additionally, the table also indicates that the DMSO condition resulted in an increase in DNA damage over the control containing no treatment. The Alkaline assay (SSBs) displays a steady increase in percentage of DNA in the tail as the concentration of camptothecin is increased. The Neutral assay (DSBs) shows a similar increase in DNA damage at lower concentrations, 10 ug/ml and below. At higher concentrations the values of percent DNA in the tail saturate and remain constant despite increases in camptothecin. The histogram of the Alkaline assay, Figure 8, shows the majority of the population of comets lie in a low DNA damage region. In Figure 9, the histogram of the Neutral assay, the data again resembles a bimodal distribution with a second peak occurring in a region of higher DNA damage.

Contractile Function:

Hydrogen Peroxide Treatments	Beats per minute	Normalized beats per minute
Control	61.91 ± 6.58	1
100 uM	68.59 ± 5.04	1.11
300 uM	50.16 ± 6.98	0.81

Table 4: *Calculated beats per minute of HL-1 cells following hydrogen peroxide treatments.*

Bleomycin Treatments	Beats per minute	Normalized beats per minute
Control	61.11 ± 5.62	1
1 ug/ml	49.38 ± 7.63	0.81
10 ug/ml	59.96 ± 14.33	0.98
50 ug/ml	37.42 ± 6.66	0.61
75 ug/ml	34.72 ± 5.41	0.57
100 ug/ml	38.99 ± 10.59	0.64

Table 5: *Calculated beats per minute of HL-1 cells following bleomycin treatments.*

Camptothecin Treatments	Beats per minute	Normalized beats per minute
Control	16.67 ± 9.22	1
DMSO	23.53 ± 4.76	1.41
1 ug ml	36.33 ± 4.55	2.18
10 ug ml	25.21 ± 6.49	1.51
50 ug ml	27.84 ± 6.12	1.67
100 ug ml	27.18 ± 5.01	1.63
200 ug ml	27.88 ± 8.64	1.67

Table 6: *Calculated beats per minute of HL-1 cells following camptothecin treatments.*

The data of contractile function for hydrogen peroxide is shown in Table 4. As compared to the control, at low levels of hydrogen peroxide, around100 uM, a slight increase in beat rate is observed. However, at high levels, around 300 uM, there is a decrease of beats per minute among the HL-1 cells. In the contractile data for treatments of bleomycin, located in Table 5, a decrease in beats per minute compared to the control is present for all conditions. However, at treatments greater than 50 ug/ml of bleomycin, a similar beat rate was observed even as concentration increased. This trend is also shown in Table 6 for treatments of camptothecin. At treatments of about 10 ug/ml and higher, a relatively equal beat rate was found. In the camptothecin conditions, the treatment of camptothecin resulted in an increase of beats per minute when compared to the control condition, with 1 ug/ml providing the greatest increase in beat rate.

Discussion

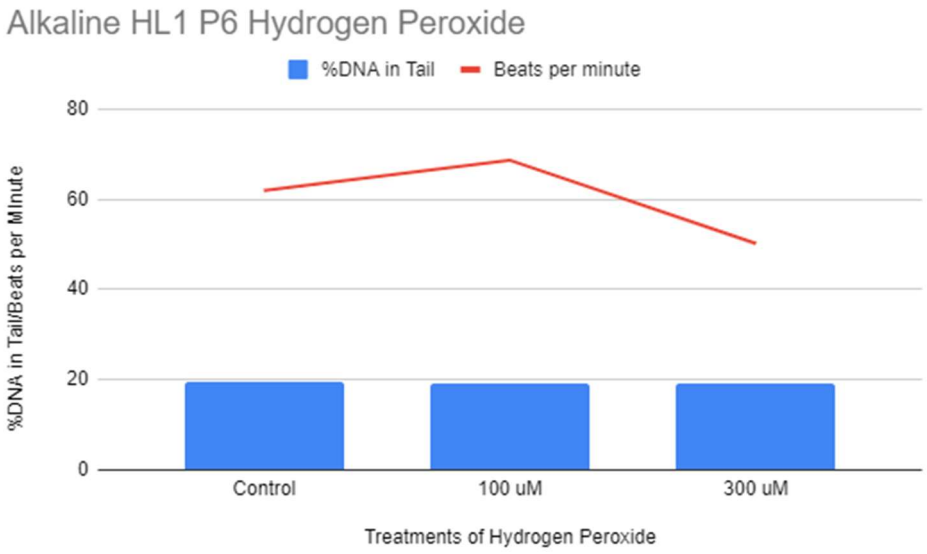

Figure 10: *Comparison of the percent DNA in tail of alkaline comets to the beats per minute calculated for hydrogen peroxide treatments.*

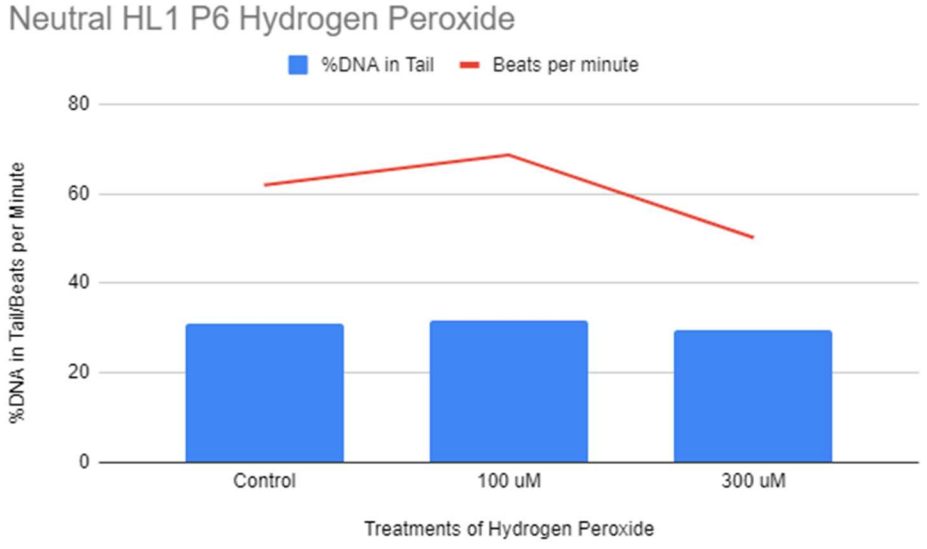

Figure 11: *Comparison of the percent DNA in tail of neutral comets to the beats per minute calculated for hydrogen peroxide treatments.*

The comparison of DNA damage and contractile function for the treatments of hydrogen peroxide is shown in figures 10 & 11 above. The increasing concentrations of hydrogen peroxide had no effect on the abundance of SSBs, shown in the alkaline assay, or the abundance of DSB, represented by the neutral assay. From these results, it can be concluded that the effects of oxidative stress on the contractile function of HL-1 cells are not caused by the induction of SSBs or DSBs. However, the increasing concentrations of hydrogen peroxide affected the contractile function. At low concentrations of hydrogen peroxide, the beat rate was seen to increase when compared to the control, representing a stimulatory effect. At high concentrations, the resulting beats per minute decreased, possibly due to hindered activity of cells due to damaged proteins or oxidative damage.

Since the presence of hydrogen peroxide still affects the resulting beat rate without increasing the abundance of SSBs and DSBs, hydrogen peroxide can be implied to act on other mechanisms within the cell that also contribute toward contractile function. This could be a consequence of oxidative damage that occurs separately from the production of SSBs and DSBs. An example of oxidative damage occurring independently would be the generation of 8-Oxoguanine (8-oxoG) base lesions. 8-oxoGs can introduce G-quadruplex folding which modifies the secondary structure of DNA, affecting cellular function. It is also possible that the oxidative stress initiates other reactions in the cell other than DNA damage, such as through signaling cascades that produce biological responses. Oxidative stress also has the potential to damage other cellular organelles such as mitochondria, and cellular components such as proteins and lipids, which would affect the function of the cell.

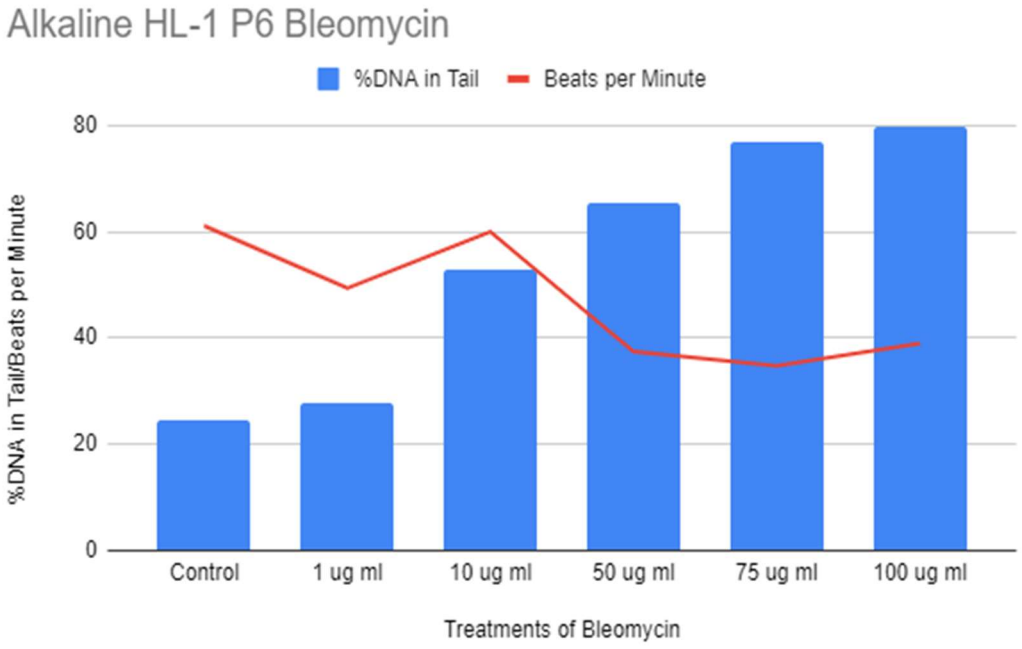

Figure 12: *Comparison of the percent DNA in tail of alkaline comets to the beats per minute calculated for bleomycin treatments.*

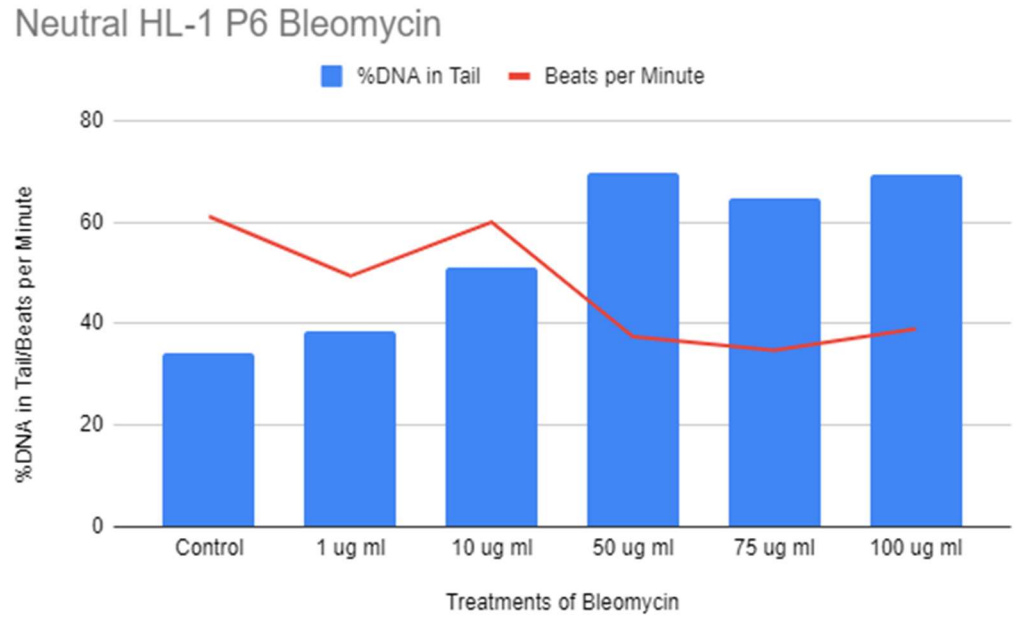

Figure 13: *Comparison of the percent DNA in tail of neutral comets to the beats per minute calculated for bleomycin treatments.*

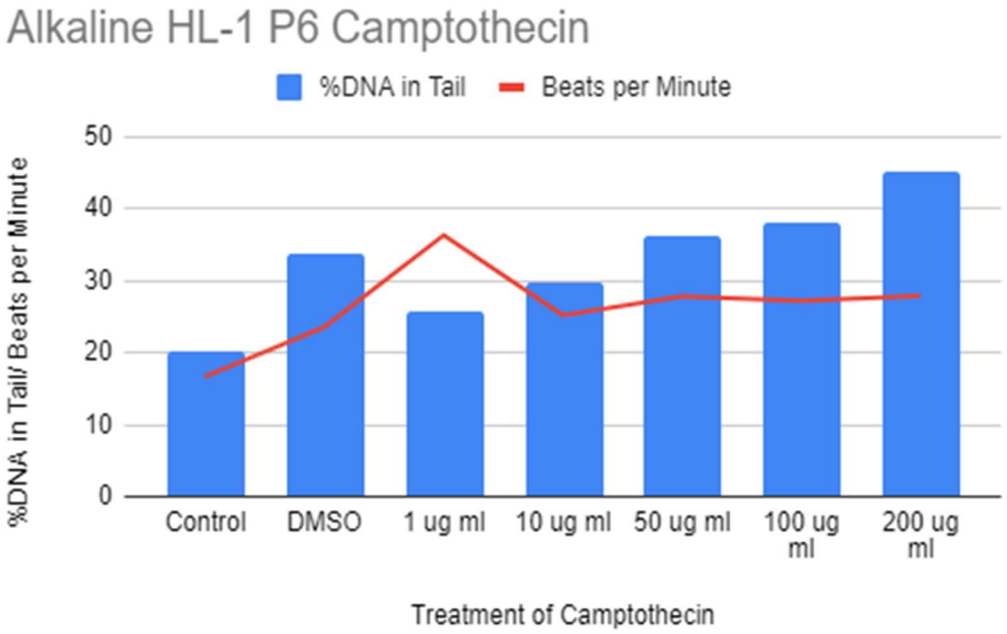

Figure 14: *Comparison of the percent DNA in tail of alkaline comets to the beats per minute calculated for camptothecin treatments.*

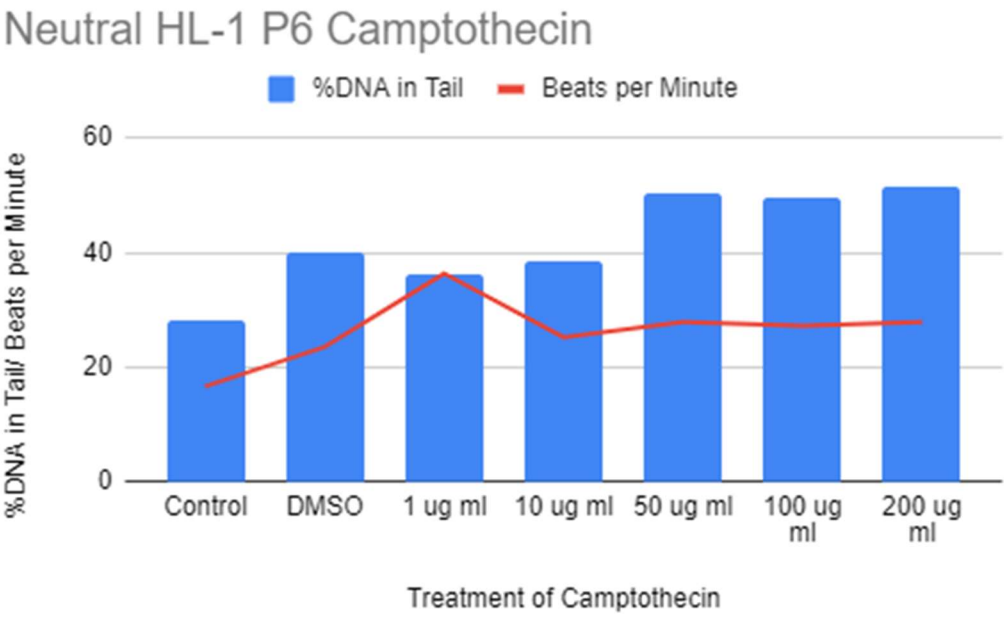

Figure 15: *Comparison of the percent DNA in tail of neutral comets to the beats per minute calculated for camptothecin treatments.*

Figures 12 & 13 and 14 & 15 reflect the comparison of percent DNA in the tail and the beats per minute found for the treatments of bleomycin and camptothecin. The increasing treatments of camptothecin corresponds to an increase in beat rate, followed by a decrease down to a beat rate that is held constant. This indicates that low concentrations of camptothecin increase the beat rate of HL-1 cells. The increase in beat rate at low concentration levels was also observed for treatments of bleomycin, with the peak in beats per minute occurring at treatment concentrations of around 10 ug/ml. Overall, these results show that the treatments for bleomycin show the beat rate obtaining a slight decrease, followed by an increase then decreasing again to a level that is held constant as the concentration increases. Future trials to repeat this conclusion would be beneficial to establish its statistical significance.

HL-1 cells are shown to exhibit a higher sensitivity to the induction of DSBs. This is displayed by reaching and maintaining the maximum level of DNA in the neutral comet assay at 50 ug/ml and above for treatments of both camptothecin and bleomycin. This indicates that lower concentrations of these two chemical reagents are sufficient to induce a higher frequency of DSBs. For comparison, the generation of SSBs steadily increased as treatment concentration increased. This shows that higher levels of a chemical reagent are necessary to attain the threshold of maximum SSB DNA damage. This occurs when increasing the treatment concentration does not produce an increase in the abundance of DNA damage, as displayed for DSB in the neutral assay.

At low concentration levels of camptothecin and bleomycin, the abundance of SSBs and DSBs (shown in alkaline and neutral comet assays, respectively) both increase as concentration increases. Therefore, the origin of the effects on contractile function cannot be differentiated between SSBs or DSBs since both follow the same trend at low treatment concentration levels.

However, at higher treatment levels, the presence of DSBs reach a threshold and become saturated. On the other hand, SSBs continue to increase as treatment concentrations are increased. This is an important difference since it allows the separation of the result of SSBs compared to DSBs to be identified. Since the beats per minute also remains unchanged at high treatment concentrations, this aligns with the trend of DSB abundance. In contrast, if SSBs were believed to have a larger influence on contractile function rather than DSBs, then the resulting beats per minute would be expected to be variable due to the steady increase in SSBs. Since contractile function remains constant while the level of DSBs are similarly invariable, then it can be interpreted that the relationship between the two are closely linked. Therefore, these results would lead to the conclusion that DSBs have a greater contribution toward contractile function than SSBs. Again, each of these conclusions would need to be verified with the addition of repeated conditions to validate statistical significance.

Future Directions

This experiment could be expanded upon by refining the treatment concentrations at low levels, prior to reaching the saturation level of DSBs. An example would be to add supplemental treatment conditions around 1, 5, 10, 15 and 20 ug/ml of bleomycin and camptothecin. This would help determine a more precise effect of low levels of treatment on the contractile function. Since the treatments of camptothecin and bleomycin both indicated an increase in beat rate at low concentration levels, exploring the precise concentration when this occurs would be beneficial. Establishing the specific outcome would be particularly useful for the treatments of bleomycin since the influence on contractile function was relatively variable from decreasing, increasing then decreasing again. This addition would be notable to clarify the trend of beats per minute as a result of increasing bleomycin concentration.

Another improvement to the experiment design would be implementing techniques to mitigate the effects of DMSO on DNA damage. DMSO was used as the solvent to dissolve bleomycin into solution for treatments. Therefore, the control condition of DMSO was used to distinguish the additional effects of DMSO from the use of bleomycin itself. In preliminary data, supplied in the appendix, DMSO introduced high levels of DNA damage. With this consideration in mind, the experiment provided above was performed with a higher concentration of stock solution. This allowed for the use of lower volumes of DMSO to minimize its effects. In this experiment, DNA damage inflicted by DMSO was lower than in the preceding data but it was still present in moderate levels. Greater efforts to eliminate this contribution, such as by exploring other solvents that are more biologically compatible with the HL-1 cells, would help isolate the results from bleomycin independently.

For the treatments of hydrogen peroxide, SSBs and DSBs were not associated with the effects on the contractile function of HL-1 cells. It would be valuable to confirm if the effects are caused by oxidative DNA damage instead. A future goal to supplement this experiment would be to measure the presence of oxidative DNA damage and compare with contractile function. This can be similarly accomplished through the implementation of a comet assay. The alkaline comet assay can be modified through the addition of a lesion-specific enzyme following lysis for the detection of 8-oxoG. Typically, a DNA glycosylase enzyme is selected due to its ability to cleave oxidized purines, including 8-oxoG. The detected abundance of oxidative DNA damage would be studied alongside the contractile data to establish their relationship [29] [30].

Another future direction would be the application of the HL-1 studies into a model system that more closely resembles the environment of a human heart. This would allow for more accurate conclusions to be drawn regarding the impact of DNA damage on cardiovascular function. One consideration would be the use of human-induced pluripotent stem cell-derived cardiomyocytes (hiPSC-CMs) to provide a human cellular model. These cells are derived by differentiating somatic cells and reprogramming them to produce pluripotent stem cells (iPSCs) [31]. The iPSCs are then differentiated into cardiomyocytes through specific media selection and supplementation of signaling molecules [32]. These cells beat spontaneously and can be visualized even in the absence of dye. Additionally, hiPSC-CMs are advantageous in studies regarding disease modeling since they maintain the affected biological phenotype of the original somatic cells [33]. It would be significant to study if the claims discovered for HL-1 cells are transferable in a human model.

These studies on the effects of oxidative stress and DNA damage on the contractile function of HL-1 cells are significant to help elucidate the mechanisms behind cardiovascular

diseases and heart failure. Unlocking the information behind the disease pathogenesis of DNA damage on contractile function would allow innovation for precisely targeted methods for therapeutics, particularly involving methods of DNA repair. It is important to explore these concepts to guide future developments in the treatment or prevention of heart disease, which is strongly related to cardiac contractility. For example, recent emphasis on the role of inflammation and oxidative stress in heart failure has presented potential therapeutic targets to be antioxidant and anti-inflammatory drugs. However, these areas are still in their infancy and require greater focus for their development [16]. The larger approach of this project was to develop a greater in-depth understanding of the factors connected to contractile function in an effort to provide a foundation for future research addressing these relevant biological questions.

Acknowledgments

I would like to thank my mentor, Dr. Colin Wu for his continuous support and guidance throughout the completion of this project. I am extremely grateful for the encouragement and invaluable knowledge and skills that I have been able to learn and develop. I would also like to acknowledge Kaitlin Lowran for her help and expertise as well as all other members of the Wu lab that have made my research experience impactful. Lastly, I would like to show my appreciation for the organizations that enabled my research to occur, thank you to the Honors College and the American Heart Association at Oakland University.

Appendix

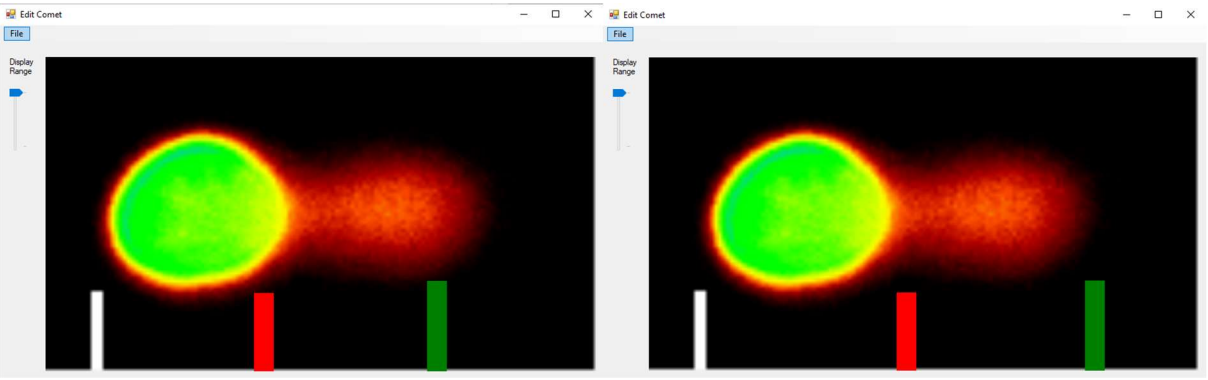

Figures 16 & 17: *When using the Trevigen comet analysis software, the parameters for the nucleus (red bar) and end of the comet tail (green bar) must be manually adjusted to ensure accuracy. The image on the left indicates the shifted bar placement when only using the software. The image on the right shows the proper placement of parameters after corrections.*

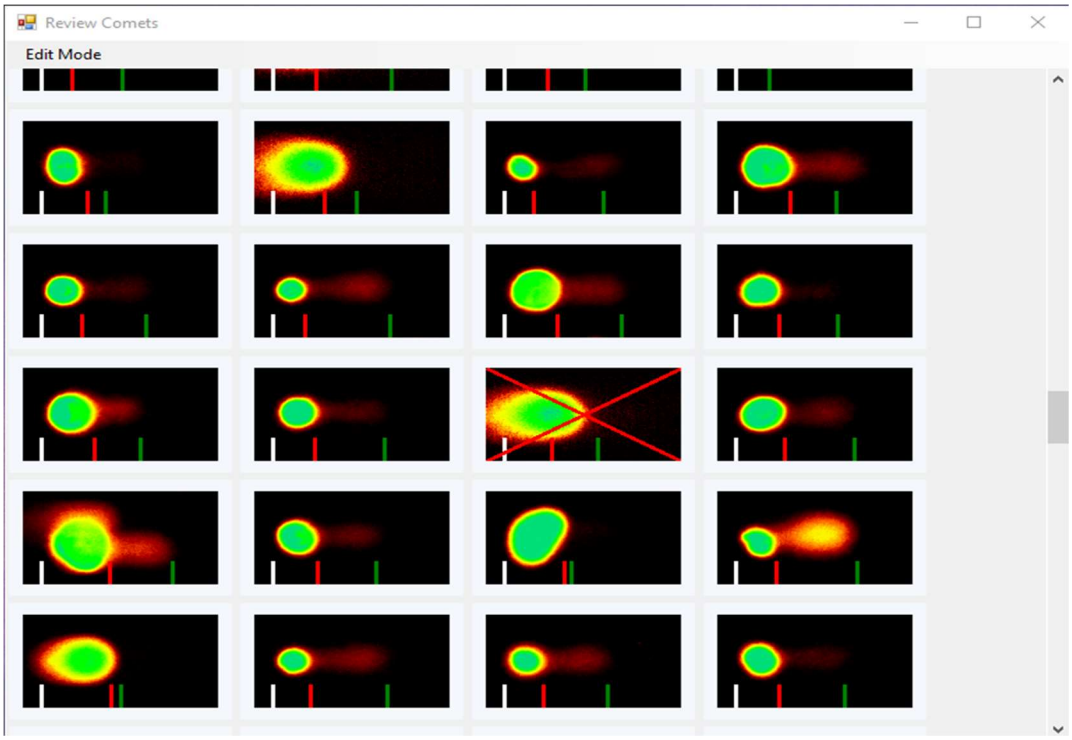

Figure 18: *The parameters of every comet must be evaluated. Comets are excluded, as shown by the red X above, if they are irregularly shaped or if there are interfering signals in the frame.*

```
%Each well of each treatment must be analyzed

%Locate peaks
findpeaks(A1, Time);
%Separate peaks based on their prominence
findpeaks(A1, Time, 'MinPeakProminence', 10000000);
%Load peak locations into an array
[pks, locs]= findpeaks(A1, Time, 'MinPeakProminence', 10000000);
%Average the differences in the location (time) between peaks
Average=mean(diff(locs))
```

Figure 19: *The matlab script used for the calculation of the average time between beats.*

$$Beats\ per\ Minute = \frac{60\ s/min}{Distance\ between\ Beats\ (s/beat)} \quad (1)$$

Equation 1: *Calculation of beats per minute using the average time between beats identified in Matlab.*

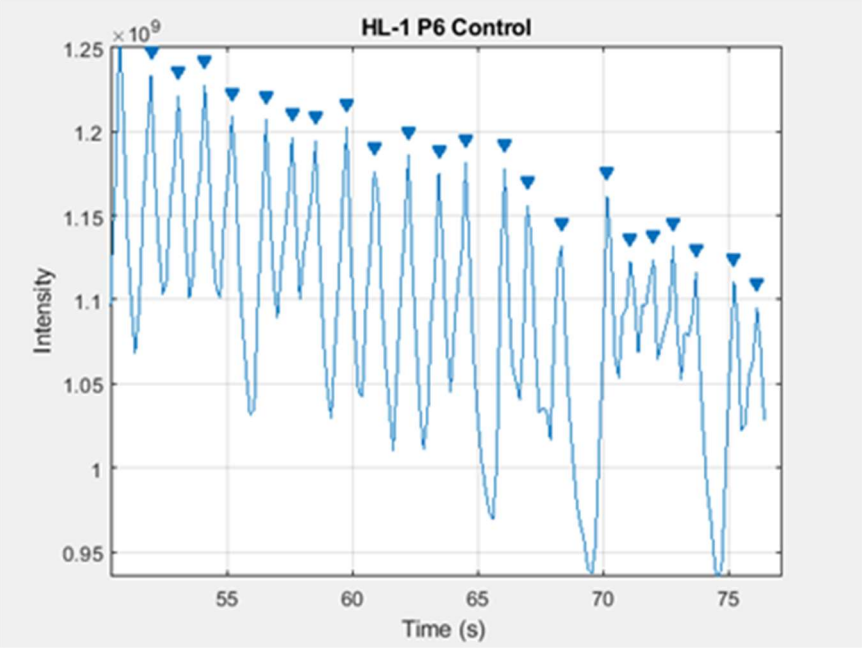

Figure 20: *Sample figure of the detection of peaks generated through Matlab.*

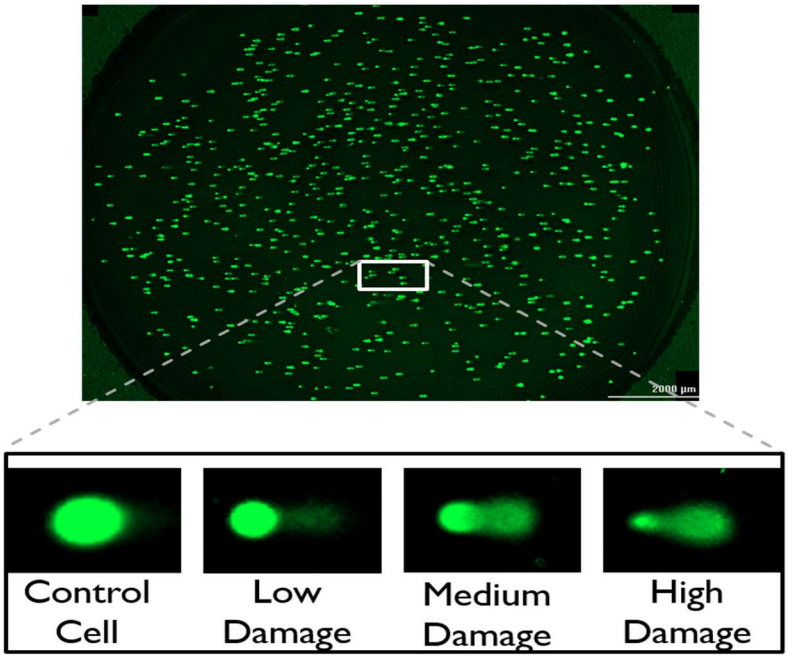

Figure 21: *Sample alkaline comet assay performed with control cells. This figure provides a reference for the expected comet shape and distribution of DNA in the tail for increasing levels of DNA damage.*

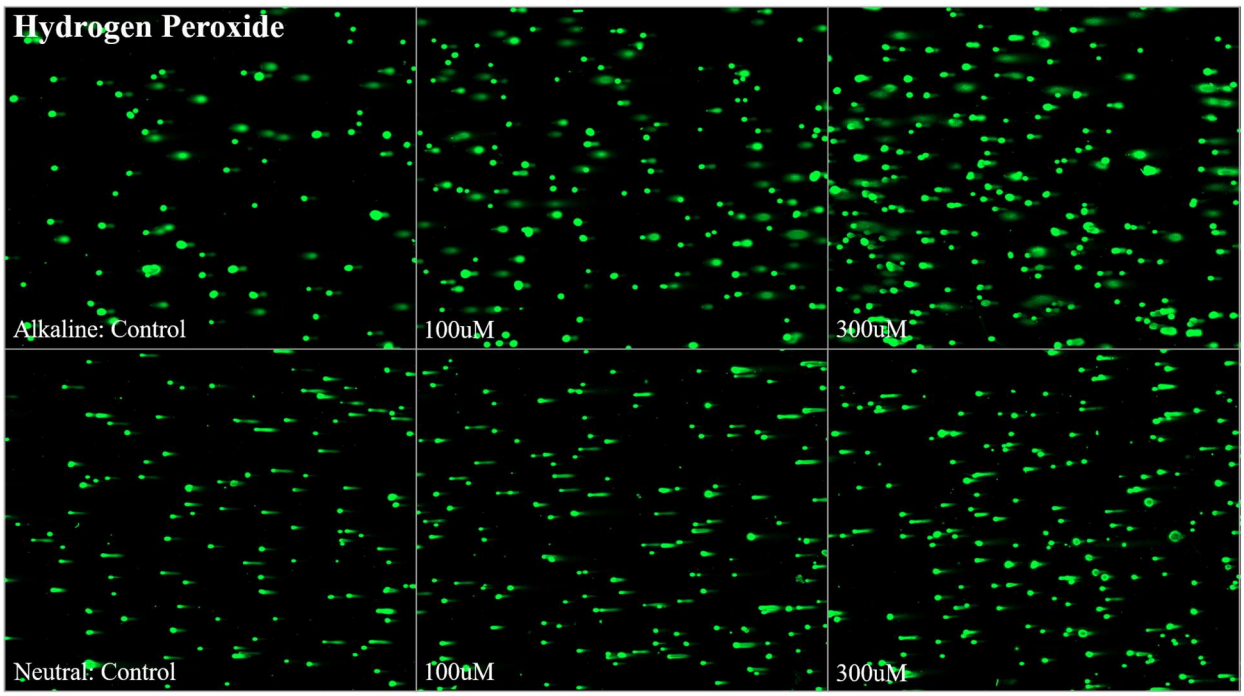

Figure 22: *Sample comet images of HL-1 cells after treatment with hydrogen peroxide.*

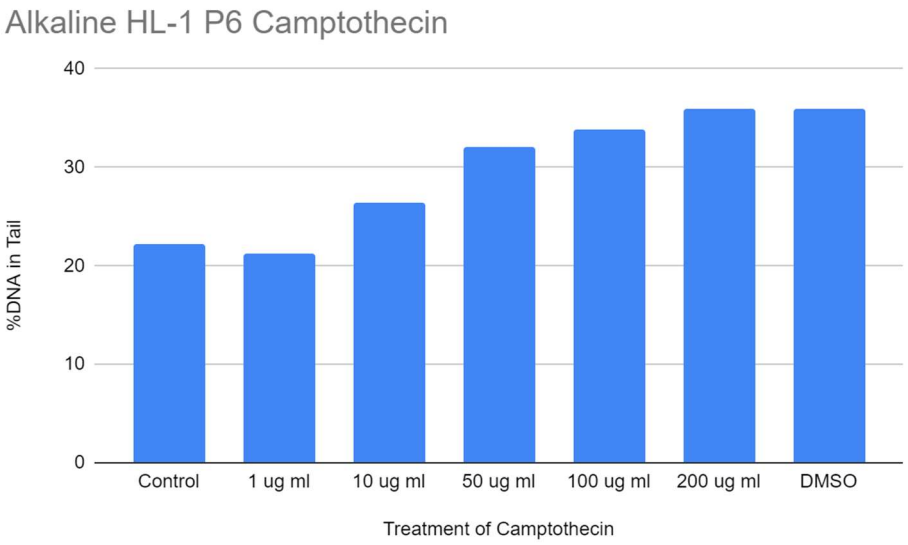

Figure 23: *Preliminary camptothecin treatments that indicate high DNA damage in the control DMSO condition for the alkaline comet.*

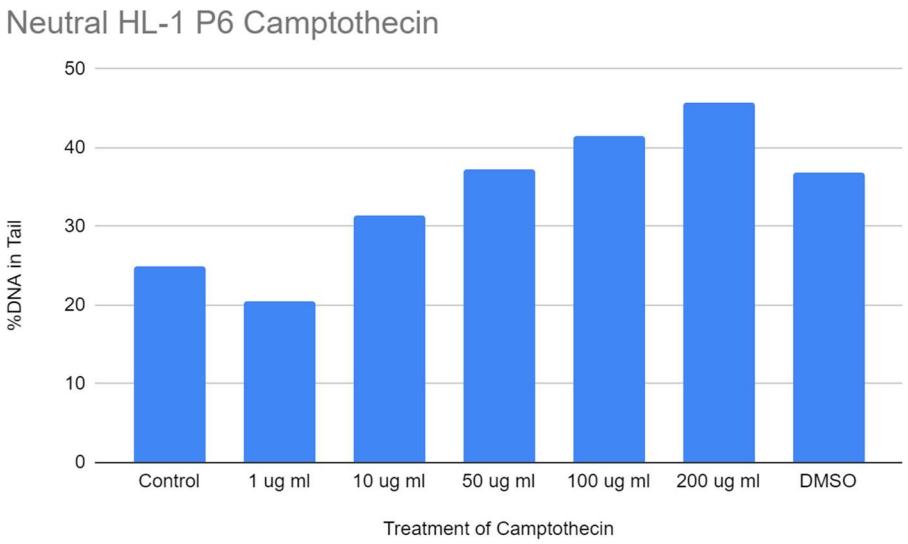

Figure 24: *Preliminary camptothecin treatments that indicate high DNA damage in the control DMSO condition for the neutral comet.*

References

1. Martin, L.J., *DNA damage and repair: relevance to mechanisms of neurodegeneration.* J Neuropathol Exp Neurol, 2008. **67**(5): p. 377-87.
2. *DNA Lesion*, in *Encyclopedic Reference of Genomics and Proteomics in Molecular Medicine*. 2006, Springer Berlin Heidelberg: Berlin, Heidelberg. p. 429-429.
3. Jackson, S.P. and J. Bartek, *The DNA-damage response in human biology and disease.* Nature, 2009. **461**(7267): p. 1071-8.
4. Caldecott, K.W., *Single-strand break repair and genetic disease.* Nat Rev Genet, 2008. **9**(8): p. 619-31.
5. Hossain, M.A., Y. Lin, and S. Yan, *Single-Strand Break End Resection in Genome Integrity: Mechanism and Regulation by APE2.* Int J Mol Sci, 2018. **19**(8).
6. Bassing, C.H. and F.W. Alt, *The cellular response to general and programmed DNA double strand breaks.* DNA Repair (Amst), 2004. **3**(8-9): p. 781-96.
7. Cannan, W.J. and D.S. Pederson, *Mechanisms and Consequences of Double-Strand DNA Break Formation in Chromatin.* J Cell Physiol, 2016. **231**(1): p. 3-14.
8. Slonczewski, J., E. Zinser, and J. Foster, *Microbiology: An Evolving Science*. 5th Edition ed. 2020: W. W. Norton & Company, Inc.
9. Poetsch, A.R., *The genomics of oxidative DNA damage, repair, and resulting mutagenesis.* Comput Struct Biotechnol J, 2020. **18**: p. 207-219.
10. Chatterjee, N. and G.C. Walker, *Mechanisms of DNA damage, repair, and mutagenesis.* Environ Mol Mutagen, 2017. **58**(5): p. 235-263.
11. Kitta, K., et al., *Hepatocyte growth factor protects cardiac myocytes against oxidative stress-induced apoptosis.* Free Radic Biol Med, 2001. **31**(7): p. 902-10.
12. Xie, J., et al., *H2O2 evokes injury of cardiomyocytes through upregulating HMGB1.* Hellenic J Cardiol, 2014. **55**(2): p. 101-6.
13. Li, Y., et al., *Corin protects H2O2-induced apoptosis through PI3K/AKT and NF-kappaB pathway in cardiomyocytes.* Biomed Pharmacother, 2018. **97**: p. 594-599.
14. Yang, W.J., et al., *Cell fusion contributes to the rescue of apoptotic cardiomyocytes by bone marrow cells.* J Cell Mol Med, 2012. **16**(12): p. 3085-95.
15. Tsutsui, H., S. Kinugawa, and S. Matsushima, *Oxidative stress and heart failure.* Am J Physiol Heart Circ Physiol, 2011. **301**(6): p. H2181-90.
16. Aimo, A., et al., *Oxidative stress and inflammation in the evolution of heart failure: From pathophysiology to therapeutic strategies.* Eur J Prev Cardiol, 2020. **27**(5): p. 494-510.
17. Zima, A.V. and L.A. Blatter, *Redox regulation of cardiac calcium channels and transporters.* Cardiovasc Res, 2006. **71**(2): p. 310-21.
18. Higo, T., et al., *DNA single-strand break-induced DNA damage response causes heart failure.* Nat Commun, 2017. **8**: p. 15104.
19. Zhang, D., et al., *DNA damage-induced PARP1 activation confers cardiomyocyte dysfunction through NAD(+) depletion in experimental atrial fibrillation.* Nat Commun, 2019. **10**(1): p. 1307.
20. Claycomb, W.C., et al., *HL-1 cells: a cardiac muscle cell line that contracts and retains phenotypic characteristics of the adult cardiomyocyte.* Proc Natl Acad Sci U S A, 1998. **95**(6): p. 2979-84.

21. White, S.M., P.E. Constantin, and W.C. Claycomb, *Cardiac physiology at the cellular level: use of cultured HL-1 cardiomyocytes for studies of cardiac muscle cell structure and function.* Am J Physiol Heart Circ Physiol, 2004. **286**(3): p. H823-9.
22. Oh, J.G., et al., *Experimental models of cardiac physiology and pathology.* Heart Fail Rev, 2019. **24**(4): p. 601-615.
23. Sakasai, R. and K. Iwabuchi, *The distinctive cellular responses to DNA strand breaks caused by a DNA topoisomerase I poison in conjunction with DNA replication and RNA transcription.* Genes Genet Syst, 2016. **90**(4): p. 187-94.
24. Decker, A., et al., *Direct hydrogen-atom abstraction by activated bleomycin: an experimental and computational study.* J Am Chem Soc, 2006. **128**(14): p. 4719-33.
25. Gunasekarana, V., G.V. Raj, and P. Chand, *A comprehensive review on clinical applications of comet assay.* J Clin Diagn Res, 2015. **9**(3): p. GE01-5.
26. Dickey, J.S., et al., *H2AX: functional roles and potential applications.* Chromosoma, 2009. **118**(6): p. 683-92.
27. Grant, A.O., *Cardiac ion channels.* Circ Arrhythm Electrophysiol, 2009. **2**(2): p. 185-94.
28. Krans, J.L., *The Sliding Filament Theory of Muscle Contraction.* Nature Education, 2010. **3**(9): p. 66.
29. Azqueta, A. and A.R. Collins, *The essential comet assay: a comprehensive guide to measuring DNA damage and repair.* Arch Toxicol, 2013. **87**(6): p. 949-68.
30. Muruzabal, D., et al., *Novel approach for the detection of alkylated bases using the enzyme-modified comet assay.* Toxicology Letters, 2020. **330**: p. 108-117.
31. Pourrier, M. and D. Fedida, *The Emergence of Human Induced Pluripotent Stem Cell-Derived Cardiomyocytes (hiPSC-CMs) as a Platform to Model Arrhythmogenic Diseases.* Int J Mol Sci, 2020. **21**(2).
32. Yoshida, Y. and S. Yamanaka, *iPS cells: a source of cardiac regeneration.* J Mol Cell Cardiol, 2011. **50**(2): p. 327-32.
33. Di Baldassarre, A., et al., *Human-Induced Pluripotent Stem Cell Technology and Cardiomyocyte Generation: Progress and Clinical Applications.* Cells, 2018. **7**(6).